Eur J Pediatr (2012) 171:1257–1263
DOI 10.1007/s00431-012-1768-7

ORIGINAL ARTICLE

Non-invasive diagnosis of lung tuberculosis in children by single voxel ^{1}H-magnetic resonance spectroscopy

Ky Santy · Phang Nan · Yay Chantana · Denis Laurent · Ianina Scheer · Beat Steinmann · David Nadal · Beat Richner

Received: 26 March 2012 / Revised: 29 May 2012 / Accepted: 30 May 2012 / Published online: 7 July 2012

Abstract Our previous study showed that ^{1}H-magnetic resonance spectroscopy (^{1}H-MRS) can detect lipid peaks characteristic for *Mycobacterium tuberculosis* infection in cerebral lesions of young children; therefore, we aimed to extend and validate the application of ^{1}H-MRS for the diagnosis of active pulmonary tuberculosis lesions in three adolescent patients. Here, we document lipid peaks characteristic for *M. tuberculosis* infection by ^{1}H-MRS from lung tissue surrounding lung cavities of two patients whose sputum samples were positive for acid-fast bacilli by microscopy and positive for *M. tuberculosis* by genetic testing, indicating active tuberculosis. A similar lipid peak was found also in the pleural effusion of a third patient with concurrent lung cavity compatible with active tuberculosis. However, in a patient with a pyogenic pulmonary abscess, ^{1}H-MRS of the drained pus displayed different characteristic peaks but no lipid peak at all. *Conclusion*: Our findings further validate ^{1}H-MRS as a rapid, non-invasive, and specific diagnostic tool for active tuberculosis in children with microbiologically documented infection outside the central nervous system, specifically in the lungs.

Keywords Pulmonary lesions · Diagnosis · Magnetic resonance imaging · Lipid · ^{1}H-magnetic resonance spectroscopy · Tuberculosis · Resource-poor country

Abbreviations

MRI	Magnetic resonance imaging
^{1}H-MRS	^{1}H magnetic resonance spectroscopy
CT	Computerized tomography
TB	Tuberculosis

Introduction

The diagnosis of tuberculosis (TB) in children is hindered compared to in adults for several reasons; these include mainly atypical clinical presentation, unspecific signs on imaging, and incapability to expectorate sputum for analysis

K. Santy · P. Nan · Y. Chantana · B. Richner (✉)
Division of Pediatrics, Jayavarman VII Hospital,
Kantha Bopha Children's Hospital,
Siem Reap, Cambodia
e-mail: beatrichner@online.com.kh

K. Santy
Division of Pediatric Imaging, Jayavarman VII Hospital,
Kantha Bopha Children's Hospital,
Siem Reap, Cambodia

D. Laurent
Division of Pediatric Laboratory Medicine and Microbiology,
Jayavarman VII Hospital, Kantha Bopha Children's Hospital,
Siem Reap, Cambodia

I. Scheer
Division of Imaging, University Children's Hospital of Zurich,
Zurich, Switzerland

B. Steinmann
Division of Metabolism, University Children's Hospital of Zurich,
Zurich, Switzerland

D. Nadal (✉)
Division of Infectious Diseases and Hospital Epidemiology, and
Children's Research Center (CRC), University Children's Hospital
of Zurich,
Steinwiesstrasse 75,
8032 Zurich, Switzerland
e-mail: david.nadal@kispi.uzh.ch

[2, 6, 9]. Therefore, tuberculin skin testing to detect delayed-type hypersensitivity or in vitro assays to detect interferon-γ release by immune cells are often used as diagnostic tools to get indirect evidence of infection with the causative agent *Mycobacterium tuberculosis*. Nevertheless, the results of both tests do not allow clear-cut distinction between active and latent infection [7].

We have recently reported on the use of ^{1}H-magnetic resonance spectroscopy (^{1}H-MRS) to detect lipid peaks characteristic for cerebral *M. tuberculosis* infection manifesting as tuberculoma in young children [8]. The ^{1}H-MRS findings in vivo and in vitro were quite similar in children in whom aspiration of lesion material was feasible, and tuberculoma uniformly exhibited elevated lipid peaks by ^{1}H-MRS and antituberculous treatment led to size reduction of the cerebral lesions exhibiting lipid peaks [8]; our findings suggested that ^{1}H-MRS may help to discriminate between various active infectious etiologies [8]. However, the application of ^{1}H-MRS to forms of TB in children other than cerebral tuberculoma has not yet been reported.

The aim of the present study was to extend and validate the application of ^{1}H-MRS for the diagnosis of active pulmonary TB lesions. For this reason, we performed ^{1}H-MRS in three adolescent patients with chest X-ray and CT findings suggestive for TB and compared them to those from a patient with a pyogenic lung abscess. All patients presented with lung cavities and the third with an additional contralateral pleural effusion. Sputum from the first two patients could be sampled for microbiological and molecular investigation. Our results further support the uniqueness of ^{1}H-MRS to establish unambiguously the diagnosis of active *M. tuberculosis* infection by non-invasive means.

Patients and methods

Patients The patients reported herein were hospitalized at Jayavarman VII, Siem Reap, one of the five Kantha Bopha children's hospitals in Cambodia, because of severe illness requiring inpatient care. Chest MRI and single voxel ^{1}H-MRS were done to investigate the reason for the marked respiratory impairment and the cause of the pathological chest X-ray and CT findings suggesting TB. A fourth patient with a pyogenic lung abscess was included for comparison.

Magnetic resonance imaging (MRI) and ^{1}H-magnetic resonance spectroscopy (^{1}H-MRS) In brief, imaging was performed on a standard 3T MR Unit (Philips Achieva 3-T, Best, the Netherlands) using an eight-channel phased-array body coil. Conventional imaging included multiplanar T1- and T2-weighted sequences as well as contrast-enhanced T1-weighted sequences of the lung covering the thorax down to the lower edge of the diaphragm. MRI was performed in

Table 1 Synopsis of demographics and findings on admission and outcome in four patients with intrathoracic lesions, three of them showing lipid peaks in ^{1}H-MRS

Case Nr.	Age (years)	Sex	Clinical signs/symptoms	Days sick	Temp (°C)	Chest X-ray/CT/MRI	WBC (G/l)	Platelets (G/l)	Puncture	Microbiological investigations	^{1}H-MRS	Outcome
1	15	f	Dyspnea, cough	10	36.5	Atelectasis and cavern upper lobe R	17.6	631	nd	Sputum: Gram stain no bacteria, AFB+, GE+, bacterial cultures negative	Lipid peak (around cavity)	Good; discharge 4 weeks; fup 3 months
2	14	m	Fever, hemoptysis	14	37.0	Cavern upper lobe R	7.7	524	nd	Sputum: Gram stain no bacteria, AFB+, GE+, bacterial cultures negative	Lipid peak (around cavity)	Good; discharge 4 weeks; under fup
3	13	m	Hemoptysis	90	38.0	Opacity hemithorax L, cavern upper lobe R	13.5	1,088	nd	NA	Lipid peak (pleural effusion)	Reasonable evolution; discharge 3 weeks; lung L partial resolution on X-rays at 5 months
4	14	f	Fever, dyspnea, cough	7	39.0	Abscess lower lobe L, infiltrates in periphery	14.4	1,194	Pus	Aspirated pus: Gram stain: Gram + cocci; culture negative[a]; AFB−, GE−	In ex vivo ^{1}H-MRS of pus: Ac, Suc, Lac, Aa peaks	Good; discharge 3 weeks, X-ray normal at 4 months

All patients were HIV negative; antimicrobial treatment consisted of ceftriaxone (10 days); metronidazole (10 days); steroids (2 weeks); plus isoniazid, rifampicin, and pyrazinamide in cases 1–3; and ceftriaxone and metronidazole for 23 days in case 4

X-ray radiography, *CT* computerized tomography, *MRI* magnetic resonance imaging, *^{1}H-MRS* magnetic resonance spectroscopy, + positive, *AFB* acid-fast bacilli (Ziehl–Neelson stain), *GE* GenExpert, *WBC* white blood cells, *fup* follow-up, *f* female, *m* male, *R* right, *L* left, *NA* not available, *nd* not done, *Ac* acetate, *Suc* succinate, *Lac* lactate, *Aa* amino acids

[a] Patient was treated with unspecified antibiotics for 1 week at home before consultation at the hospital

free breathing without respiratory gating (acquisitions in axial, sagittal, and coronal plans). These sequences were done for the evaluation of anatomical lesions. Single voxel ^{1}H-MRS was performed using a point resolved excitation selective spectroscopy sequence (PRESS) prior to the contrast-enhanced sequence using the standard departmental sequences as recently published [8]. Specifically, the imaging parameters were repetition time (TR)=2,000 and echo time (TE)= 35 ms or 144 ms in order to differentiate lipid peaks (0.9–1.3 ppm) from the overlapping lactate peak (1.3 ppm), respectively. The number of acquisitions was 128 resulting in an effective ^{1}H-MRS acquisition time of 4 to 5 min. The voxel was positioned within the lesion of interest. To avoid potential respiratory motion artifacts and inclusion of lesions located too peripherally, the patient had to stay still in a quiet breathing condition during a timed acquisition. The voxel was manually positioned within the lesion or the pleural fluid, and its size was optimized for the size of the lesion or the pleural effusion. In lesions with air–fluid level, the volume of interest (VOI) was mandatorily located in the full-fluid collection of the cavity, thus avoiding air–fluid-related artifact that could disturb ^{1}H-MRS spectra. The acquired data were postprocessed using the vendor-specific software. The metabolites were displayed along the typical resonance frequency axis at which the typical lipid peaks appear at 0.9–1.3 ppm. In addition, in vitro ^{1}H-MRS was performed of the aspirated pus as described recently [8].

Laboratory investigations Blood counts, chemistry, bacterial cultures, and species identification, as well as human immunodeficiency virus (HIV) serology, were done using routine hospital procedures and methods.

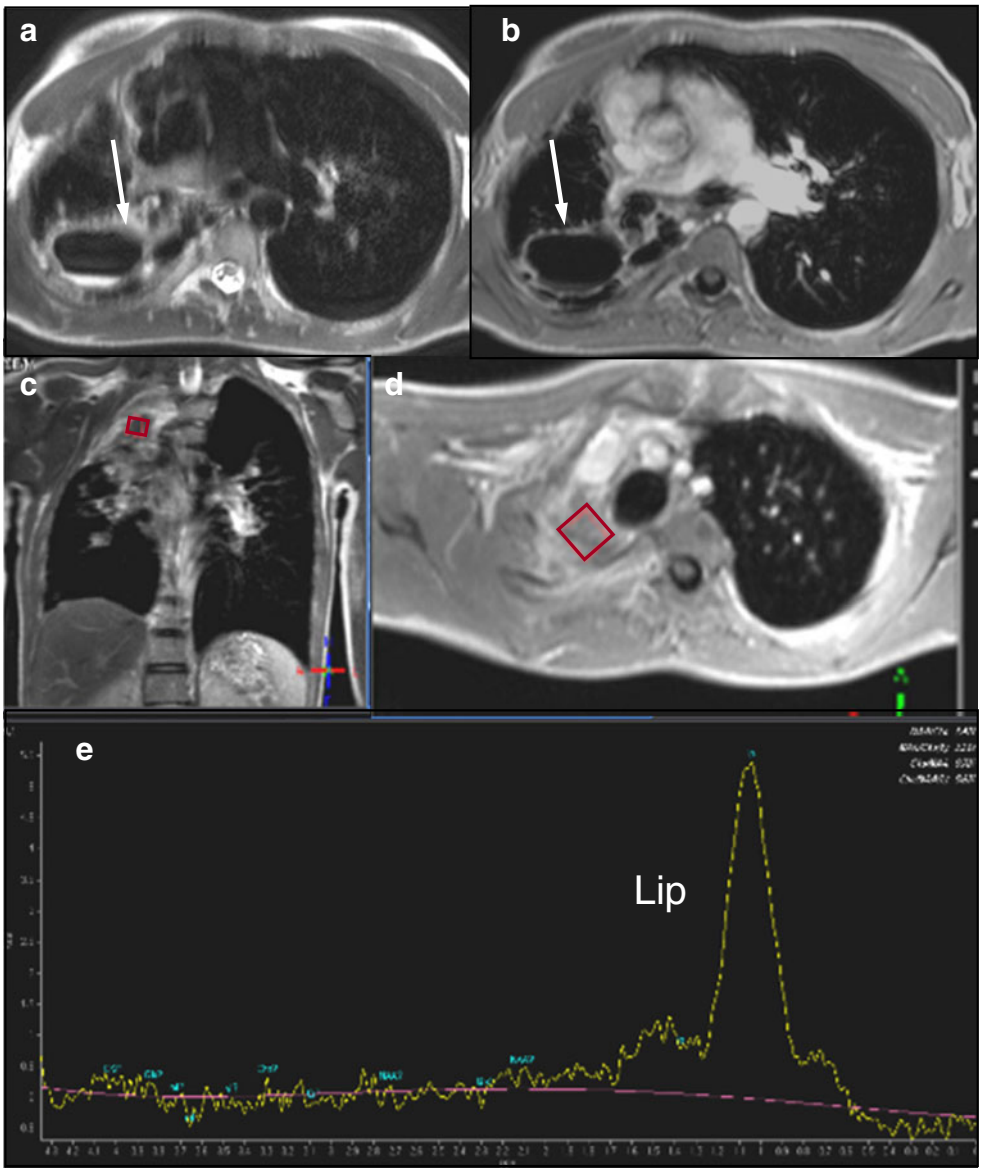

Fig. 1 Case 1: Axial T2 (**a**) and axial contrast-enhanced T1-weighted (**b**) MR images reveal a large pulmonary cavern in the right posterior upper lobe (*white arrow*). ^{1}H-MRS (**e**) of the upper lobe consolidation cranial to the cavern shows a broad lipid (*Lip*) peak at 0.9–1.3 ppm. The *rhombus symbols* indicate the voxel position of the ^{1}H-MRS (**c**, **d**)

Molecular detection of M. tuberculosis Nucleic acid of *M. tuberculosis* in sputum was detected using GenExpert (Cepheid, Sunnyvale, CA, USA) according to the instructions of the manufacturer. This test detects also rifampicin resistance that is a surrogate for multi-drug resistance.

Clinical assessment The clinical status was evaluated in all patients prior, during, and after treatment.

Results

A synopsis of the demographic, clinical, imaging, spectroscopic, and laboratory findings as well as the course of the patients reported here is given in Table 1. The patients were 13 to 15 years old, and their histories of acute illness were characterized by fever, cough, dyspnea, hemoptysis, or weight loss and had lasted 7 to 90 days. Three patients showed signs of cavern formation in the upper right lung lobe, and one of them presented in addition with a left-sided pleural effusion. One patient had leukocytosis (>15 G/l), all patients had thrombocytosis (>500 G/l), and all were HIV negative.

The two older patients with cavities were able to expectorate, and sputum from both was negative for bacteria on Gram staining and bacterial cultures, but was positive for acid-fast bacilli and for molecular detection of *M. tuberculosis* using GenExpert (Table 1; cases 1 and 2) that further excluded rifampicin resistance. No sputum or pleural effusion was obtained from the third patient (Table 1; case 3). In these three patients, ^{1}H-MRS revealed elevated lipid peaks in the pulmonary consolidations surrounding the cavities (case 1: Fig. 1 and case 2: Fig. 2) as well as in the pleural fluid (case 3: Fig. 3). Notably, cases 1 and 2 presented well-organized lesions as intra-parenchymal round cavities that

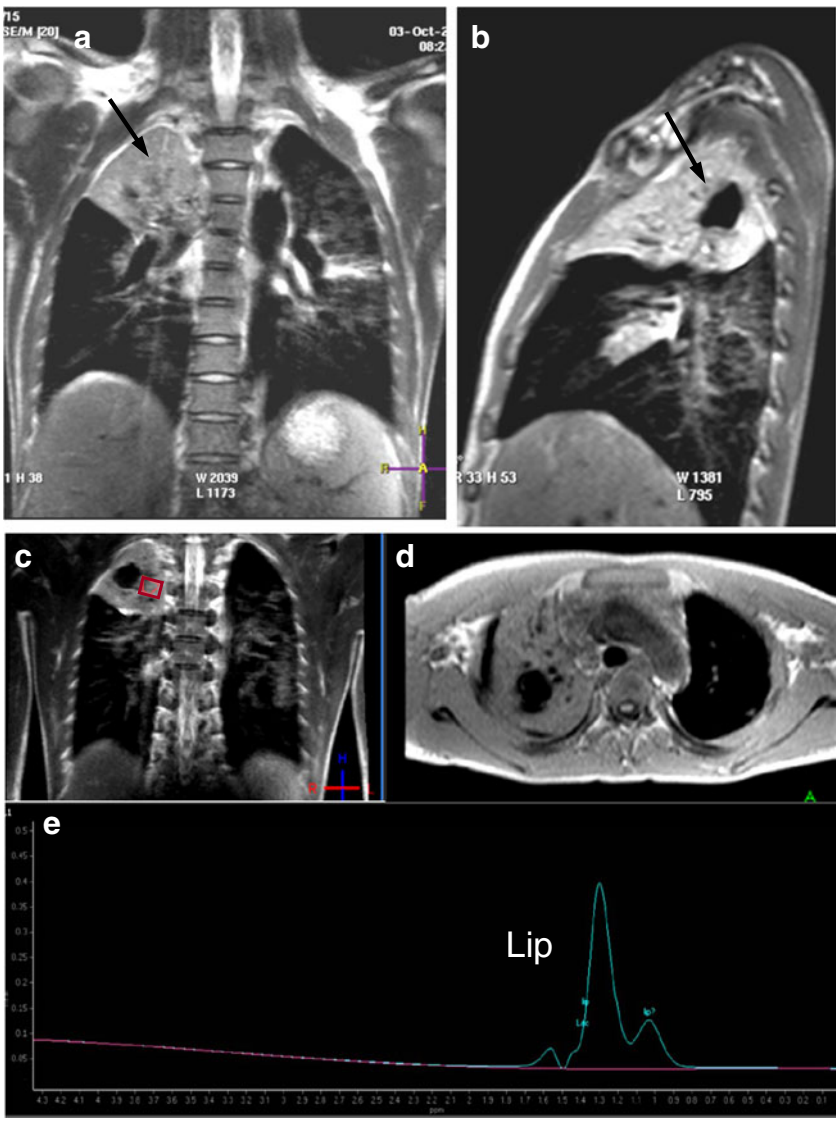

Fig. 2 Case 2: Coronal (**a**), sagittal (**b**) T2-weighted, and axial T1-weighted (**d**) MR images reveal a large pulmonary cavern in the apex of the right upper lobe within a large consolidation (*black arrow* in **a**, **b**). ^{1}H-MRS (**e**) within the consolidation shows lipid (*Lip*) peaks at 1.0 and 1.3 ppm, respectively. The *rhombus symbol* indicates the voxel position of the ^{1}H-MRS (**c**)

were well separated from parahilar vessel structures that could disturb ^{1}H-MRS. Case 3 showed fluid collection in the left pleural cavity with consolidation of the adjacent lung parenchyma, and an air-cavern lesion in the right upper lobe; in this case, ^{1}H-MRS was not possible in the air-filling cavity and consolidation area due to artifacts caused by air and blood flow. Nevertheless, ^{1}H-MRS was possible in the left pleural effusion. In cases 1–3, by CT, there were no detectable calcifications that could disturb ^{1}H-MRS. Treatment included isoniazid, rifampin, and pyrazinamide for 6 months, ceftriaxone, and metronidazole for 10 days, and steroids for 2 weeks, all medications in dosages adjusted to age and weight. These three patients were discharged in good conditions after 3–4 weeks, and follow-up for at least two more months showed a favorable clinical course (Table 1).

Case 4 showed an abscess in the lower left lobe. The aspirated pus contained Gram-positive cocci that did not grow in bacterial cultures, probably because of antibiotic pretreatment. Furthermore, acid-fast staining and GenExpert assay were negative. ^{1}H-MRS ex vivo, as done previously [8], showed acetate, succinate, lactate, and amino acid peaks (Table 1; Fig. 4). Treatment with ceftriaxone and metronidazole was terminated after 23 days, and the patient was discharged after 3 weeks in good conditions.

Discussion

While ^{1}H-MRS allows to identify brain tuberculoma non-invasively with high specificity [8], we set out to apply and validate this technique also for the diagnosis of active

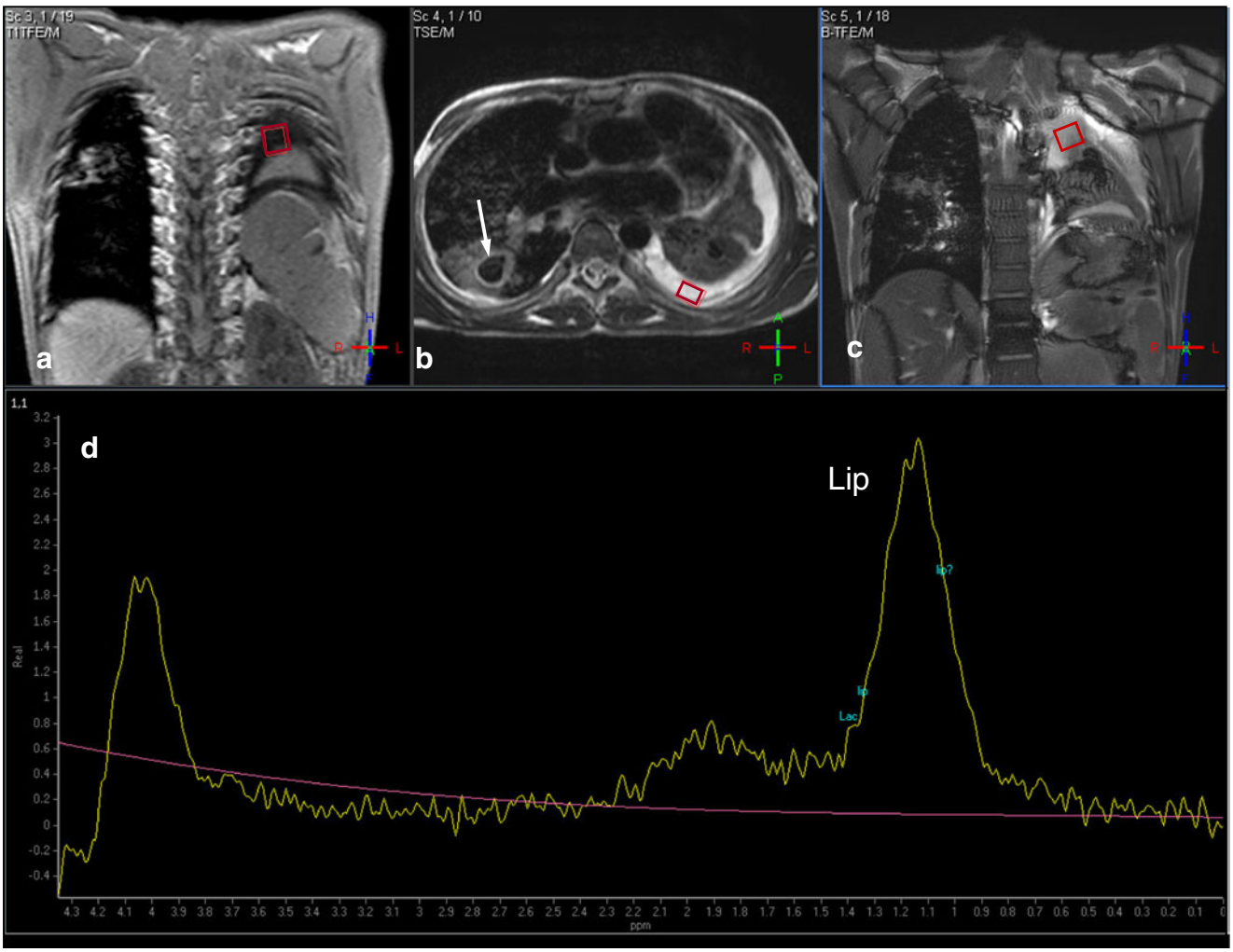

Fig. 3 Case 3: Coronal T1 (**a**), axial (**b**), and coronal (**c**) T2-weighted images show a cavern in the right lung (*white arrow* in **b**) and the atelectatic left lung and large pleural effusion on the left (*black arrow*). ^{1}H-MRS of the effusion (**d**) shows a broad lipid (*Lip*) peak at 0.9–1.3 ppm. Note the residual water peak at 4.0–4.2 ppm due to poor shimming. The *rhombus symbols* indicate the position of the voxels of the ^{1}H-MRS (*black arrow*)

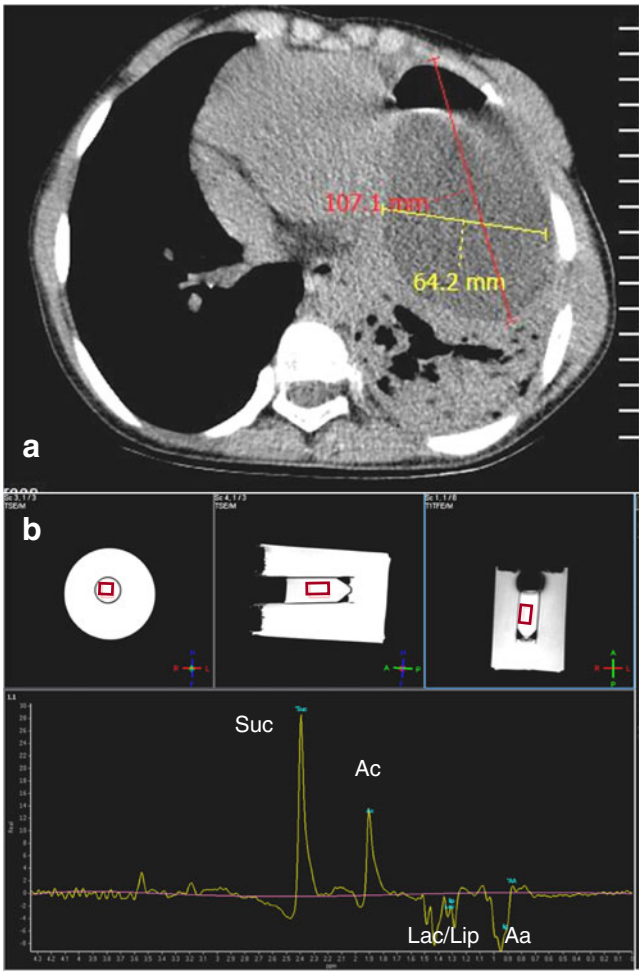

Fig. 4 Case 4: Axial CT (**a**) showing an abscess in the lower left lobe. ^{1}H-MRS of the aspirated pus (**b**) shows large acetate (*Ac*) and succinate (*Suc*) peaks as well as small lactate/lipid (*Lac*/*Lip*) and amino acid (*Aa*) peaks. The spectrum was taken at TE 144 ms as opposed to TE 35 ms used for spectra in Figs. 1, 2, and 3. *Rhombus symbols* show the voxel position of the ^{1}H-MRS

pulmonary TB lesions. We found lipid peaks characteristic for active *M. tuberculosis* infection in ^{1}H-MRS [3, 4, 8] in three patients with suspected TB: in two patients with lung cavities whose sputum samples were positive for acid-fast bacilli and for genetic testing of *M. tuberculosis* and in one patient with a pleural effusion. Hence, we show ^{1}H-MRS lipid peaks in children with microbiologically established TB and thus further validate ^{1}H-MRS as a specific non-invasive diagnostic tool for active TB in children.

^{1}H-MRS within the chest is challenging because of moving lung, pulsating vessel structures, and air. To avoid artifacts caused by neighboring air or vascular structures, the voxel must be positioned in a well-defined fluid collection. ^{1}H-MRS may be less affected by respiration-related motion in the upper pulmonary lobes where TB preferentially localizes. If multiple lesions are present, the voxel should be set in the largest solid lesion and not within an air-filled cavity. Since we allowed the patients to breath during acquisition time, the spectrum could be undetermined or not interpretable; in such case, the acquisition was repeated to obtain unequivocal data. Thus, careful positioning of the voxel and immediate quality assessment of the spectrum obtained are crucial.

The clear-cut lipid peaks visualized by ^{1}H-MRS in three adolescents presenting with lung cavity formation were striking. Subsequent detection of acid-fast bacilli and the genetic identification of *M. tuberculosis* in sputum of two of the patients allowed to firmly establish the diagnosis of active TB and robustly validated the diagnostic value of the lipid peaks detected in the lungs. Notably, ^{1}H-MRS in the three patients did not show any of the additional acetate, succinate, lactate, or amino acid peaks. This suggested that conventional bacteria were not involved in the lung abscesses [3, 8], and indeed, staining and culture of sputum for conventional bacteria were negative. Undeniably, pyogenic lung abscess as confirmed by Gram staining lacked the lipid peak but showed acetate, succinate, lactate, and amino acid peaks, strikingly contrasting our observation in the three other patients. Thus, ^{1}H-MRS seems to be a rather specific diagnostic tool to differentiate lung lesions due to *M. tuberculosis* from those caused by pyogenic bacteria.

The demonstration of a lipid peak in ^{1}H-MRS of pleural effusion in case 3, being very similar to those detected in pulmonary consolidations surrounding microbiologically and genetically confirmed tuberculous lung lesions in cases 1 and 2, is remarkable. The absence of peaks other than the lipid peak in ^{1}H-MRS again argues against conventional bacteria being the cause of the pleural effusion [5]. Moreover, the contralateral cavity formation in the lung was suggestive of active TB [5, 6]. Therefore, in view of the favorable course in the patient subsequent to antituberculous treatment, active TB seems very likely. Thus, it is tempting to speculate that ^{1}H-MRS may be useful to diagnose active TB even in pleural effusion.

Our report has the limitation that cases 1–3 received ceftriaxone and metronidazole together with the antituberculous regimen in the initial 10 days of treatment. Both antimicrobials are active against conventional bacteria that may cause lung or pleural pathology, and they were prescribed empirically since no data on the specificity of ^{1}H-MRS from lungs were available so far. Thus, the favorable responses of the patients to the installed antimicrobial treatment could also be due to the action of ceftriaxone or metronidazole, or both. The negative staining and cultures for conventional bacteria and the absence of acetate, succinate, lactate, and/or amino acid peaks in ^{1}H-MRS, however, make this unlikely [5].

In summary, ^{1}H-MRS was validated for the non-invasive establishing the diagnosis of active TB in microbiologically confirmed tuberculous lung cavity lesions and provides also a powerful, rapid, specific, and sensitive tool to diagnose TB

manifesting pleural effusion. Importantly, ^{1}H-MRS must be considered in the close context of clinical and imaging findings [2] since lipid peaks may not be entirely specific for TB in conditions including tissue necrosis [1]. Albeit ^{1}H-MRS may be regarded as a method to be reserved for high-technology medical facilities in wealthy countries, our report evidences that it may provide an excellent, non-invasive tool to improve significantly medical care and cure of TB in areas where this is of paramount importance.

Acknowledgments The Kantha Bopha Foundation that is supported by donations, mainly from Swiss people, made this study possible. The authors thank Prof. Thierry A. Huisman for helpful discussions.

Conflict of interest The authors declare that they have no conflict of interest.

References

1. Chang L, Ernst T (1997) MR spectroscopy and diffusion-weighted MR imaging in focal brain lesions in AIDS. Neuroimaging Clin N Am 7:409–426
2. Cuevas LE, Browning R, Bossuyt P, Casenghi M, Cotton MF, Cruz AT, Dodd LE et al (2012) Evaluation of tuberculosis diagnostics in children: 2. Methodological issues for conducting and reporting research evaluations of tuberculosis diagnostics for intrathoracic tuberculosis in children. Consensus from an expert panel. J Infect Dis 205(Suppl 2):S209–S215
3. Gupta RK, Vatsal DK, Husain N, Chawla S, Prasad KN, Roy R, Kumar R, Jha D, Husain M (2001) Differentiation of tuberculous from pyogenic brain abscesses with in vivo proton MR spectroscopy and magnetization transfer MR imaging. AJNR Am J Neuroradiol 22:1503–1509
4. Luthra G, Parihar A, Nath K, Jaiswal S, Prasad KN, Husain N, Husain M, Singh S, Behari S, Gupta RK (2007) Comparative evaluation of fungal, tubercular, and pyogenic brain abscesses with conventional and diffusion MR imaging and proton MR spectroscopy. AJNR Am J Neuroradiol 28:1332–1338
5. Marais BJ, Raviglione MC, Donald PR, Harries AD, Kritski AL, Graham SM, El-Sadr WM, Harrington M, Churchyard G, Mwaba P, Sanne I, Kaufmann SH, Whitty CJ, Atun R, Zumla A (2010) Scale-up of services and research priorities for diagnosis, management, and control of tuberculosis: a call to action. Lancet 375:2179–2191
6. Marais BJ, Schaaf HS (2010) Childhood tuberculosis: an emerging and previously neglected problem. Infect Dis Clin North Am 24:727–749
7. Rangaka MX, Wilkinson KA, Glynn JR, Ling D, Menzies D, Mwansa-Kambafwile J, Fielding K, Wilkinson RJ, Pai M (2012) Predictive value of interferon-gamma release assays for incident active tuberculosis: a systematic review and meta-analysis. Lancet Infect Dis 12:45–55
8. Santy K, Nan P, Chantana Y, Laurent D, Nadal D, Richner B (2011) The diagnosis of brain tuberculoma by (1)H-magnetic resonance spectroscopy. Eur J Pediatr 170:379–387
9. Swaminathan S, Rekha B (2010) Pediatric tuberculosis: global overview and challenges. Clin Infect Dis 50(Suppl 3):S184–S194